Effects of Distributed Generation on Carbon Emission Reduction of Distribution Network

Di Wu[1], Jun Su[1,2,*], Zhengyu Chen[1] and Hanhan Liu[1]

[1]*School of Electrical Engineering and Automation, Xiamen University of Technology, Xiamen, China*
[2]*Xiamen Key Laboratory of Frontier Electric Power Equipment and Intelligent Control, Xiamen, China*
E-mail: junsu1989@163.com
[*]*Corresponding Author*

Received 17 June 2023; Accepted 24 August 2023;
Publication 02 November 2023

Abstract

Increasing renewable energy integration in power systems is an important way of decarbonising carbon emissions. Recently, the ever-increasing deployment of distributed generation (DG) is considered effective in reducing carbon emissions and power loss, such as wind, photovoltaic (PV), and combined heat and power generation (CHP) on the demand side. Thus, the evaluation of carbon emission flow (CEF) will be a crucial factor for distribution network planning with the integration of DGs, which may act as a supplemented indicator in addition to traditional power flow study. In the planning stage, it is paramount to ensure that decarbonisation process of the power distribution system is in line with environmental and technical targets. Thus, the paper proposes a modelling strategy to combine the power flow

Distributed Generation & Alternative Energy Journal, Vol. 39_1, 57–82.
doi: 10.13052/dgaej2156-3306.3913

and carbon emission flow. It aims to analyse and calculate the CEF based on the power-flow study. The novel model satisfies the power flow and CEF balance and can be directly used to evaluate the decarbonization of power system. The results of this study can help relevant energy decision-makers to do appropriate renewable energy generation planning and guide the power system to achieve carbon neutrality.

Keywords: Distributed generation, power flow, carbon emission flow, decarbonization, carbon neutrailty.

1 Introduction

Since distributed power generation is characterised by instability and high volatility, carbon emissions of power system will also change with the fluctuation of distributed power generation. Therefore, statistics and analysis of carbon emissions are particularly important in verifying the carbon sources and carbon flows. Carbon emission in power system refers to carbon dioxide emissions mainly caused by conventional power production from coal-fired and gas-fired power plants. However, distributed renewable energy, such as wind power, Photovoltaic (PV), can effectively reduce the dependence on fossil energy and corresponding carbon dioxide emissions [1]. In addition, hybrid energy systems containing a variety of distributed renewable energy sources have also been vigorously developed, and hybrid energy systems can reduce CO_2 emissions more effectively than traditional energy systems [2, 3]. Existing methods for measuring carbon emission can be classified into statistical methods [4], input-output analysis (I-O) methods [5], and life cycle analysis (LCA) methods [6].

The energy and environmental performance of thermal power plants has been assessed widely using statistical methods and input-output analysis (I-O) methods. However, the focus in most of the statistical methods is based on continuous emission monitoring system that is used to measure CO_2, SO_2 and NOx emissions as per kWh electricity generated [1, 7]. The study [8] and [9] adopted macro energy statistics frequently suffer from mission and inconsistency flow. Generally, the statistical data only provide the numerical records of related fossil energy. It may be used to evaluate the carbon emission of a specific power plants, but can not be further developed to a universal model to evaluate carbon emission in a systematic prospective.

The life cycle assessment (LCA) on carbon emission footprint includes all environmental impacts associated with the product's entire life. The LCA was often used to evaluate carbon emission of renewable generation in which no direct carbon emission is produced during its operation. Most of the existing research conducted carbon emission evaluation that only aims at generators in coal-fired and gas-fired power plants, while ignoring the carbon emissions from demand side. Although, the distributed generation, such as solar power, at demand side, does not directly emit carbon dioxide in its operation, but its manufacturing process does produce certain carbon emission.

The study [10, 11] developed a comprehensive bottom-up life cycle assessment model to evaluate the carbon emission of solar power [10]. It indicated that life cycle GHG emissions range from 98.3 to 149.3 gCO_2/kWh, with a mean value of 123.8 gCO_2/kWh. The life cycle emission model of solar power provide an insight to evaluate the carbon footprint among power system, so as to reflect the environmental impacts of utility-scale solar project in an more objective way.

Since the electrical carbon emission is determined by the operation state of distribution networks, a detailed analysis of carbon emissions can be carried out based on the operation and manufacturing stages. Further, the electrical carbon emission of the demand side can be clarified. In order to be able to track carbon footprint and accurate carbon emission data, carbon emission flow theory is used to describe dynamic carbon emission data distributed in the power system.

The name was first proposed in the trading system for measuring the transfer of carbon between two trading parties [12]. Similar to an energy flow generated by energy generation, transfer and consumption in the power system, carbon emission can also be described as a flow. Therefore, a carbon tracking model has been established to describe the change of carbon emission with energy consumption in the power system [13]. Due to the different carbon reduction intensity of each distributed power supply, the decarbonisation process of distribution network is also different. For distribution network with high volatility of distributed power supply, the carbon emission flow can better describe their decarbonisation process. Based on the power system model with nodes and loads of distributed power supply, precise carbon emission flow is calculated in the form of network topology.

Thus, considering the impacts of DGs on carbon emission reduction, this paper proposes an improved CEF method. It can further clarify the CEF distribution in the distribution network of complex operation states.

Three contributions are as follows:

- Analyze DGs' impacts on the CEF from three aspects of the direct carbon emission source: the network power flow, network carbon intensity and network carbon flow;
- Propose an improved CEF model considering DGs' impacts to measure the carbon emissions and carbon intensity of each node within distribution networks;
- Quantify the complex CI of distribution network with multiple DGs, by innovatively combining the CI and historical CEF information;

The remainder of this paper is organized as follows. Section 2 presents the detail of the improved CEF method. In Section 3, the case study is conducted to verify the feasibility of the proposed method. Finally, conclusions are presented in Section 4.

This paper presents a modelling technique to analyse the decarbonisation process of distribution network combined with carbon emission flow. By comparing the carbon emissions of distributed power sources added with different carbon emission intensities with those provided by the main network, the carbon reduction advantages of distributed power sources are highlighted. First, the Newton-Rafson AC model was established to calculate the power flow of the distribution network continuously, and the continuous power flow distribution was obtained. Secondly, the parameters of PV power generation system and cogeneration is analysed and obtained. Then, according to the CEF calculation formula, the continuous CEF data of distribution network are obtained and compared.

2 Methodology

2.1 Power Flow Calculation Model

In the distribution network, since the carbon emission flow is dependent on the energy flow, the distribution of energy flow in the distribution network should be calculated in advance before calculating the carbon emission flow value table. On the basis of the known energy flow distribution, each carbon emission flow index is calculated. In the proposed CEF model, Newton-Raphson algorithm is integrated into matpower toolbox [14] to calculate the power flow. If there are N nodes in the distribution network, the voltage amplitude V_i and angle of each node can be calculated by the active and

reactive power balance Equations (1) and (2) of the nodes [15].

$$\mathrm{P_{Gi}} - \mathrm{P_{Li}} = \mathrm{U_i} \sum_{\mathrm{j}=1}^{\mathrm{N}} \mathrm{U_j}(\mathrm{G_{ij}} \cos \delta_{\mathrm{ij}} + \mathrm{B_{ij}} \sin \delta_{\mathrm{ij}}) \tag{1}$$

$$\mathrm{Q_{Gi}} - \mathrm{Q_{Li}} = \mathrm{U_i} \sum_{\mathrm{j}=1}^{\mathrm{N}} \mathrm{U_j}(\mathrm{G_{ij}} \sin \delta_{\mathrm{ij}} - \mathrm{B_{ij}} \cos \delta_{\mathrm{ij}}) \tag{2}$$

In the above formula, $\mathrm{P_{Gi}}$ and $\mathrm{Q_{Gi}}$ respectively represent the active and reactive power input by the generator at node i of the power system network, $\mathrm{P_{Li}}$ and $\mathrm{Q_{Li}}$ respectively represent the active and reactive power of the load at node i of the power system network, $\mathrm{G_{ij}}$ and $\mathrm{B_{ij}}$ respectively represent the conductance and susceptance of branch i-j of the distribution network. $\mathrm{U_i}$ and $\mathrm{U_j}$ represent the voltage amplitudes of nodes i and j at both ends of branch i-j of the distribution network. is the difference of voltage angle between nodes i and j at both ends of branch i-j of distribution network, which can be expressed as $\delta_{\mathrm{ij}} = \delta_{\mathrm{i}} - \delta_{\mathrm{j}}$.

$$\mathrm{P_{i-j}} = \mathrm{V_i V_j}(\mathrm{G_{ij}} \cos \delta_{\mathrm{ij}} + \mathrm{B_{ij}} \sin \delta_{\mathrm{ij}}) \tag{3}$$

$$\mathrm{P_{lossi-j}} = 2\mathrm{U_i U_j G_{ij}} \cos \delta_{\mathrm{ij}} \tag{4}$$

In the above formula, $\mathrm{P_{i-j}}$ is the active power of branch i-j in the distribution network, and the direction is i-j. $\mathrm{P_{lossi-j}}$ is the active power lost in branch i-j in the distribution network, and its direction is also i-j.

2.2 Carbon Emission Flow Model

2.2.1 Definition of main indicators of CEF

The carbon emission flow (CEF) is generated and transferred to the load side in the same way as the energy flow in the distribution network. It is defined as the carbon dioxide equivalent emission corresponding to the energy flow flowing through the network, and the unit of CEF is tCO_2.

Carbon emissions, like energy flows are continuous. Therefore, the definition of carbon emission flow rate (CEFR) describes the instantaneous carbon emission rate flowing through a network node or branch. It represents the carbon emission corresponding to the energy flow flowing through a branch or node in the power network within a unit time. The units are tCO_2/h.

In order to connect carbon emission flow with energy flow, carbon emission intensity (CI) is defined as the carbon emission generated by power generation side caused by node consumption of unit electricity within unit time [13]. The unit is tCO_2/MWh or gCO_2/kWh.

2.2.2 The original CEF model

According to the carbon emission flow model of the power system proposed in literature [16], the CEF index of the power system can be obtained by understanding the carbon emission degree of each generating unit and the energy flow distribution in the power distribution network, and then calculating the carbon emission degree of nodes.

The CEF model is established in the distribution network. Suppose there are N nodes, L branches and K generators in the network. The most important indicators of CEF are generator injection CI, generator injection CEFR, branch CEFR, load CEFR and node CI(NCI). Branch CEFR consists of the CEFR flowing through the branch and the loss CEFR of the branch.

Among them, the solving process of CEF model in [13] shows that NCI is the core calculation index.

$$\mathrm{R_{G,t}} = \mathrm{P_{G,t}E_{G,t}} \tag{5}$$

$$\mathrm{R_{i-j,t}} = \mathrm{P_{i-j,t}diag(E_{NCI,t})} + \mathrm{P_{lossi-j,t}diag(E_{NCI,t})} \tag{6}$$

$$\mathrm{R_{L,t}} = \mathrm{P_{L,t}E_{NCI,t}} \tag{7}$$

$$\mathrm{E_{NCI,t}} = \mathrm{P_{N,t}^{-1}P_{G,t}E_{G,t}} = \mathrm{(P_{N,t} - P_{i-j,t})^{-1}R_{G,t}} \tag{8}$$

$$\mathrm{P_{N,t}} = \mathrm{diag}\left(\mathrm{ones}(1, \mathrm{K+N}) \cdot \begin{bmatrix} \mathrm{P_{i-j,t}} \\ \mathrm{P_{G,t}} \end{bmatrix}\right) \tag{9}$$

The carbon emissions generated by the Equation (7) node load can be calculated as follows:

$$\mathrm{C_{L,t}} = \sum_{\mathrm{t=1}}^{\mathrm{T}} \mathrm{R_{L,t}}\Delta\mathrm{t} \tag{10}$$

Where $\mathrm{R_{G,t}}$ is the CEFR injected by the generator in time t; $\mathrm{R_{i-j,t}}$ is the CEFR of branch i-j in time period t; $\mathrm{R_{L,t}}$ is the CEFR generated by the load in time period t; $\mathrm{R_{G,t}}$, $\mathrm{R_{i-j,t}}$ and $\mathrm{R_{L,t}}$ both have units of tCO_2/h; $\mathrm{P_{G,t}}$ is the generating power of the generator in time period t; $\mathrm{P_{i-j,t}}$ is the power on

branch i-j in time period t; $P_{lossi-j,t}$ is the loss power on branch i-j in time period t; $P_{L,t}$ is the power of the load in time period t; $E_{G,t}$ is the generator injection CI, the unit is gCO_2/kWh; $C_{L,t}$ is the total carbon emission, the unit is tCO_2; $R_{G,t}$, $E_{NCI,t}$ and $C_{L,t}$ are both N-dimensional column vectors; $P_{G,t}$ is a $K \times N$ level matrix; $P_{G,t}$ is a K dimensional column vecto; $R_{i-j,t}$, $P_{i-j,t}$, $P_{lossi-j,t}$ and $P_{N,t}$ are both N level square matrices; $R_{L,t}$ and $P_{L,t}$ are both N-1-dimensional column vectors; The"diag()"denotes the diagonal matrix operator; The "ones(1,K+N)" means to set up a 1 by K plus N level matrix with all 1's.

2.2.3 Improved carbon emission flow model considering DGs' Impacts

DGs provides power directly to customers, which changes tidal energy and CEF in the distribution network. DGs most directly affects the four variables $P_{G,t}$, $E_{G,t}$, $P_{i-j,t}$, $P_{lossi-j,t}$ and $P_{N,t}$ in CEF model. Accordingly, the new generator injection CEFR, load CEFR, Branch CEFR and NCI need to be recalculated according to Equations (5)–(9). As NCI is the core index of CEF, the influence of DGs on it is deduced in detail by Equations (11)–(14). Suppose m DGs generate power at time t.

The $P_{G,t}$ change to $P'_{G,t}$ and $E_{G,t}$ change to $E'_{G,t}$ expressed as:

$$P'_{G,t} = \begin{bmatrix} P_{G.t} \\ P_{DGs,t} \end{bmatrix}, \quad E'_{G,t} = \begin{bmatrix} E_{G.t} \\ E_{DGs,t} \end{bmatrix} \tag{11}$$

Where $P_{DG,t}$ is a $m \times N$ level matrix and $E_{DG,t}$ is m dimensional column vectors; $P_{i-j,t}$ and $P_{lossi-j,t}$ recalculate the power flow to get $P'_{i-j,t}$ and $P'_{lossi-j,t}$; The new $R'_{G,t}$, $P'_{N,t}$ and $E'_{NCI,t}$ can be represented as:

$$R'_{G,t} = P'_{G,t}E'_{G,t} \tag{12}$$

$$P'_{N,t} = \mathrm{diag}\left(\mathrm{ones}(1, K+N) \cdot \begin{bmatrix} P'_{i-j,t} \\ P'_{G,t} \end{bmatrix}\right) \tag{13}$$

$$E'_{NCI,t} = P^{-1}_{N,t}P'_{G,t}E'_{G,t} = (P'_{N,t} - P'_{i-j,t})^{-1}R'_{G,t} \tag{14}$$

This study mainly analyzes the influence of DGs on carbon emissions in distribution network. It can be seen from the above formula that the size of carbon emissions has a direct relationship with NCI. This relationship is a positive correlation, that is, carbon emissions increase as NCI increases

or carbon emissions decrease as NCI decreases. To measure the impact of DG on the carbon emission of distribution network is to measure the impact of DG on the NCI of distribution network. NCI is the core index to be calculated first, and all CEF index calculations need to be completed with the participation of NCI. But, the calculation of NCI is complicated and requires many parameters, among which generator injection CI is the most important one. This is because the distribution network itself does not produce carbon emissions, and all carbon emissions are injected by generators and flow to each node along with the power flow. The CI of DG's analysis is detailed in the next section.

2.3 CI Calculation of DGs

DG is a power generation device fueled by clean energy. It can be installed directly on the demand side to provide clean energy directly to the user, which can reduce the highly polluting energy in the distribution network.

PV mainly converts solar energy into electricity, which does not involve the emission of fossil fuels. Carbon emissions generated by PV are mainly concentrated in the production link ($\mathrm{N_{PV}}$), transportation link (T) and scrap link (W) [17]. CHP generates electricity through the combustion of natural gas, which is a relatively low-carbon fossil energy. When electricity generated by traditional renewable energy sources such as PV and wind is scarce, CHP plays an important role as a stable power source [18]. CHP generates electricity through the combustion of natural gas, which is a relatively low-carbon fossil energy. The carbon emissions generated by CHP are obtained from the combustion of natural gas.

The carbon emission formula of PV and CHP is as follows:

$$\mathrm{C_{PV}} = \mathrm{N_{PV}C_P} + \mathrm{T} + \mathrm{W} \tag{15}$$

$$\mathrm{C_{CHP}} = \mathrm{V_N I_C} \tag{16}$$

Where $\mathrm{C_{PV}}$ and $\mathrm{C_{CHP}}$ respectively represent total carbon emissions of PV and CHP,the unit is tCO_2; $\mathrm{N_{PV}}$ is the carbon emissions generated per unit of power in the production of PV; $\mathrm{C_P}$ is the total power used in the production of PV; $\mathrm{V_N}$ is the volume of natural gas consumed,the unit is m^3; $\mathrm{I_C}$ is the carbon emission factor of natural gas,the unit is MJ/m^3.

PV power generation system is basically exposed to the external environment, and its components are affected by the adverse external environment,

and the power generation efficiency will decline year by year in the whole power generation life cycle. In a CHP power generation system, natural gas is burned to produce high-temperature and high-pressure steam or gas, which is used to generate electricity through thermal energy conversion equipment. PV power generation model and CHP power generation model are as follows:

$$\mathrm{E_{PV,toal}} = \mathrm{eHP_{PV}} \sum_{\mathrm{f=1}}^{25} (1 - \mathrm{B_f}) \tag{17}$$

$$\mathrm{E_{CHP,toal}} = \mathrm{V_N Q_N} \eta_\mathrm{t} \tag{18}$$

Where $\mathrm{E_{PV,toal}}$ and $\mathrm{E_{CHP,toal}}$ respectively represent total power generation of PV and CHP, the unit is kWh; e is the efficiency of PV power generation system; H is the annual effective illumination time of the region; f is the service life of PV power generation system,the maximum service life is 25 years; $\mathrm{P_{PV}}$ is the power of PV power generation system; $\mathrm{B_f}$ is the efficiency decay rate of the volt generation system in the f year; $\mathrm{Q_N}$ is natural gas of higher heating value,the unit is MJ/m^3; η_t is the efficiency of thermoelectric conversion equipment.

To sum up, the CI of the ith DGs($\mathrm{E_{i,DGs}}$) can be calculated by the following formula:

$$\mathrm{E_{i,DGs}} = \frac{\mathrm{C_{i,DGs}}}{\mathrm{E_{i,DGs}}} \tag{19}$$

The calculation parameters required to solve the CI of DGs show different values due to the economic impact of different countries and regions. Table 1 shows the CI reference values and some fixed parameters of PV and CHP. Other parameters should be calculated according to the characteristics of the local area. The specific CI value and other parameters should be calculated according to the actual local conditions.

Table 1 CI parameters of DGs

DG	CI parameters
PV	CI:123.8gCO_2/kWh, e:80%, $\mathrm{B_f}$:2%
CHP	CI:525gCO_2/kWh, $\mathrm{I_C}$:55–65g/m^3 $\mathrm{Q_N}$:35–45 MJ/m^3, η_t:15–20%

2.4 Solve the CEF Distribution in Continuous Time

Carbon emissions are produced all the time, so it is necessary to calculate carbon emissions at a given time. In this paper, the online continuous power flow scheduling policy is used to solve the problem of online energy flow distribution in the distribution network. This problem can be used to calculate the energy flow distribution under the condition of adding DG into the distribution network within a given time range, which provides a basis for solving the CEF of the distribution network including DG. As shown in Table 2, in time t, the online scheduling policy is calculated for a relatively short future time range Ht. At subsequent points $\mathrm{t}+1, \mathrm{t}+2, \ldots, \in \mathrm{T}$, the power flow calculation is performed repeatedly, and the result calculated in the first step is used as the basis for CEF calculation each time. Figure 1 shows the flow chart of calculating CEF indicators by the online continuous power flow scheduling policy, as specified in the following steps:

1. Initaly, a period of T (24 h) is divided into 96 of equal-size time intervals $\mathrm{t} \in \mathrm{T}$. Also, the three sets of knowledge.
2. Next, model the network and set up the generator and load data in the network, as well as the impedance of the network.
3. Calculate the CI of DGs. Then, run the power flow in order to get the branch power distribution in the distribution network.
4. NCI is calculated by combining branch power,generator injection CI and other indexes.then other CEF indexes were calculated by combining CEF formula.
5. Finally, move to the next time slot and repeat executing branch power and NCI until reaching the end of time scale.

Table 2 Computation flowchart CEF data in continuous time

Calculate the CEF data policy in continuous time
Basic data for continuous power flow in distribution network
$\{\mathrm{P_{Gi,t}}, \mathrm{Q_{Gi,t}}, \mathrm{P_{Li,t}}, \mathrm{Q_{Li,t}}, \mathrm{G_{i-j,t}}, \mathrm{B_{i-j,t}}\}$
Procedure
Set $\mathrm{t} \rightarrow 0$
Iterate
$\mathrm{P_{i-j,t}}$ is calculated based on power flow
Calculate the CEF data based on $\mathrm{P_{i-j,t}}$
Set $\mathrm{t} \rightarrow \mathrm{t}+1$
Output:CEF data of distribution network in a certain period of time

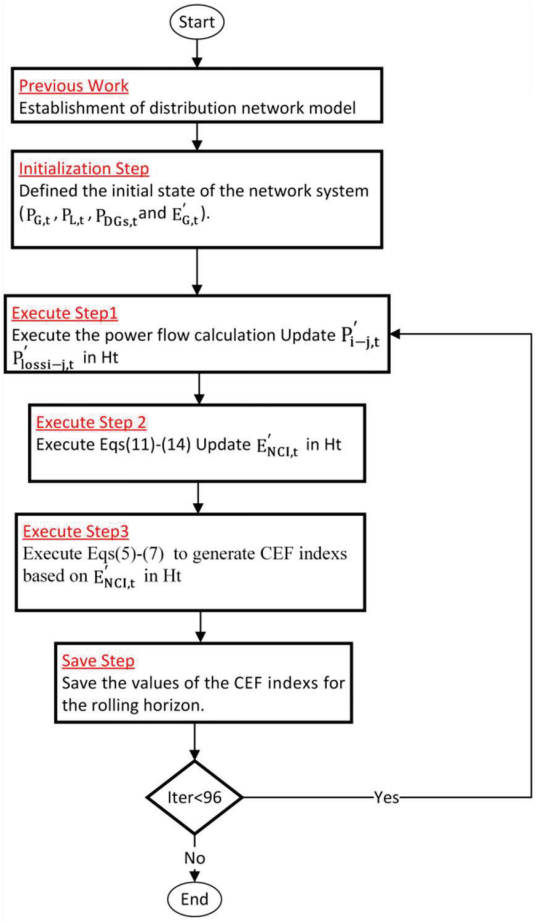

Figure 1 CEF indexs calculation flowchart.

3 Case study

3.1 IEEE 13-node System

The IEEE 13-node system is modified and simulated to verify the CEF method with the added DGs. Figure 2 gives the modified system. The system has 1 primary generator, 2 DGs and 12 branches. A total of 12 nodes carry load. The electricity-carbon model has been built up in Matlab 2019b. MATPOWER toolbox is adopted in the system to execute optimal power flow calculation at a fast convergent speed [14]. Other basic data can be obtained from MATPOWER.

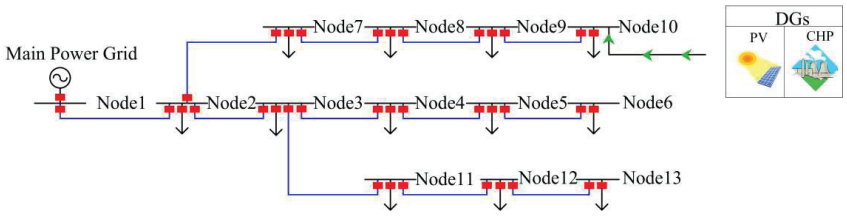

Figure 2 The modified IEEE 13-node system with DGs.

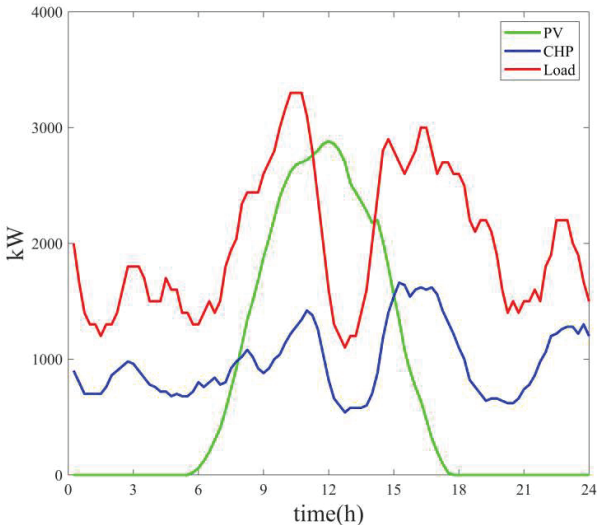

Figure 3 Typical daily power profiles of load, PV and CHP power output at node-10.

The electric carbon model has three generators generating carbon emissions, one in the main grid of node 1, and the other two are DGs (PV and CHP) set at node 10. The CI of DGs is given in Table 1, and the CI of the main power grid is 875gCO_2/kWh.

The typical daily profile of load and daily output profiles of PV and CHP at the node 10 are shown in Figure 3. The maximum and minimum power values of the load during the day are approximately 3500 kW and 1000 kW. The PV power output starts at 6:00 and ends at 17:00, the maximum output power is 3500 kW. The CHP can maintain uninterrupted power output throughout the day, the maximum and minimum power values are approximately 1600 kW and 400 kW.

The following four scenarios are simulated to analyse the uncertainty of PV power output and different generation mixes on the calculated CEF indexs

results. The case is studied within an entire day with 15 min as the interval of a time step.

- Case Study 1: Deterministic case with base loads;
- Case Study 2: Deterministic case with base loads + PV;
- Case Study 3: Deterministic case with base loads + CHP;
- Case Study 4: Deterministic case with base loads + PV + CHP;

3.2 Results and Analysis Figures

3.2.1 Simulation results of CI

To provide a clear picture of the renewable generation's impact in terms of carbon emission profile in distribution network, along the entire day, the NCI for the first three cases is compiled and presented in Figure 4. It can be found that the system NCI of Case 1 remains in 875gCO_2/kWh in a whole day, because CEF of all nodes within the system is provided by the main power grid through the node 1. With the integrating PV in Case 2, renewable power injected to the load at node 10 results in a substantial NCI reduction, which drops NCI from 875gCO_2/kWh to roughly 150gCO_2/kWh at 12:00 a.m. when PV reaches its max power generation. In Case study 3, the deployment of CHP slightly lower NCI index and keep it fluctuating all day long as the power generated from CHP is consistent and will not be curtailed for the weather reason. As these three case studies indicate that the carbon emissions

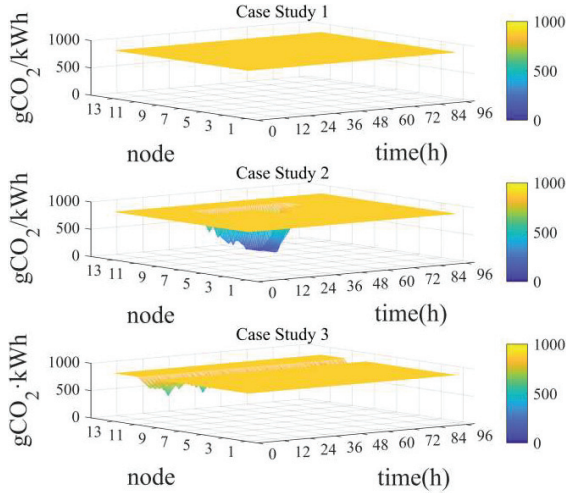

Figure 4 NCI profile of modified IEEE 13-node system with three case studies.

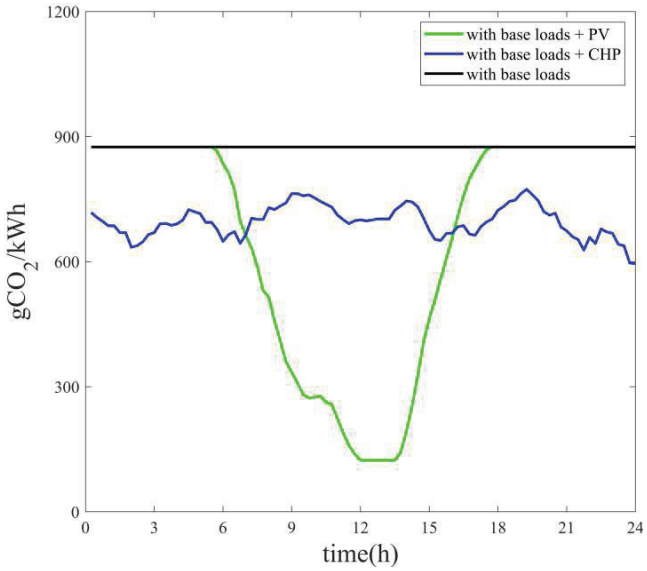

Figure 5 NCI profile at node 10 with three case studies.

of the system is directly related to amount of power injected from DGs, and the reduction extent is related to the CI and output power of DGs.

In order to assess the impact of CI brought by DGs, node 10 in Figure 2 is chosen for the analysis of three case studies. The typical daily power loads and daily DGs' ower generation are depicted in Figure 3 above. The 24-hour NCI of noe 10 is shown in Figure 5. In the case 1 with base loads only, power flow is transferred from the main power grid to power load at node 10, therefore, carbon emission also flows in the same path along with power flow. Therefore, the 24-hour CI of noe 10 is consistent with the that of the main power grid. Once PV is installed at node 10 in case study 2, loads are partially supplied by PV and main power grid respectively. Meanwhile, in the contrast to high CI of the main power grid, the low CI power generated from PV contribute to lower NCI of at node 10. Similarly, as shown in Figure 5, the deployment of CHP at node 10 also makes NCI reduced by injecting power, ever though the CI of CHP 525gCO_2/kWh is higher than that of PV 123.8gCO_2/kWh, but still lower than that of the main power grid 875gCO_2/kWh. The results demonstrate that the one of the most effect way to decrease NCI at particular node of the system is to deploy DGs and the reduction extent of NCI was also related to the CI of DG and its installed capacity.

3.2.2 Simulation results of CEFR

It can be concluded from the above section that the CI at node 10 has been reshaped by the integration of DGs. From the system point of view, the CI(gCO_2/kWh) shall be multiplied by power flow to illustrate the flowing mass of carbon emissions. Thus, the NCI at node 10 and the CEFR of branch 9-10 is taken as example to investigated carbon emission flows with the consideration of power flows.

As for branch 9-10, the direction from noe 9 to node 10 is deemed to positive. Figure 6 shows the daily CEFR of branch 9-10. The blue, green, and black curves are dedicated three cases studies respectively.

In case study 1 (black lines in Figure 6), the power flowing within branch 9-10 is all coming from main grid. Thus, branch 9-10 has the same CI as the main power grid, branch CEFR only follows the change of power flow. While in case study 2 (green lines in Figure 6), in the period of 0 a.m.to 6 a.m., the PV at node 10 is in the off state. The CEFR of branch 9-10 is kept the same as that of case study 1. However, from 6 a.m., PV gradually generates power into node 10, then, the power coming from the main grid through branch 9-10 begins to decrease. From this time on, the branch CEFR that comes from the main grid gradually begins to decrease. In the period between 12:00 a.m. to 14:00, the PV power output exceeds the power consumption of the loads at node 10. PV power begins to be transferred in reverse direction, which

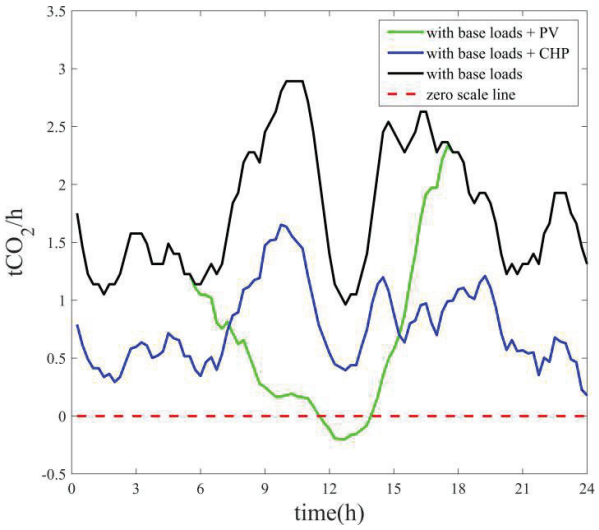

Figure 6 Change of daily branch CEFR of branch 9-10.

make power flows from node 10 to node 9. Thus, the branch CEFR becomes negative during this period. This indicates that the CEFR of branch 9-10 in this period is provided by PV, and this period is also the lowest branch CEFR in the whole day. From 14:00 to 18:00, the output power of PV begins to decrease. During this period, the branch CEFR increases gradually as the power at node 10 is provided by main grid again. From 18:00 to 24:00, PV do not produce any power at all. During this period, the branch CEFR of branch 9-10 is completely provided by the main power grid. In case study 3, the blue curves in figure shows that the CEFR of branch 9-10 is lower than that of the branch CEFR in case study 1, and the direction is from node 9 to node 10. This indicates that the branch CEFR of branch 9-10 is maintained by the main power grid and CHP, but the power generated from CHP dilute the high CI of the main power grid, resulting in branch CEFR fluctuated from 1-1.5tCO_2/h.

3.2.3 The change in NCI of node 9

From the analysis of case study 2 above, it can be seen from Figure 6 that from 12:00 to 14:00, the PV output power exceeds the power consumption of the load, and the excess PV power is feeding back to the grid through node 10 to node 9. As shown in Figure 7, near 12:00, excess renewable PV power is injected into grid along branch 9-10, leading to −1700 kW power flow in

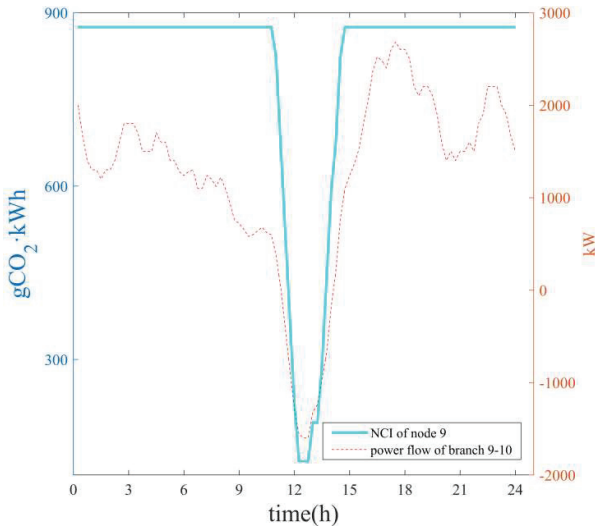

Figure 7 Change of NCI of node 9 and power flow of branch 9-10.

branch 9-10. The large amount of low-carbon power rapidly reduces the NCI to roughly 123.8gCO_2/kWh at node 9. From 12:00 to 13:00, the load power of node 9 is completely provided by PV, so that the NCI of this time period is the same as that of PV, and the carbon emissions of this time period is also the lowest in the whole day. In the following period, with the decrease of PV output power, NCI of node 9 began to rise, and recovered to the original value when PV power completely disappeared. The results show that when the power of DGs is large enough, its low carbon power can be transferred to the nearby load and reduce the carbon emission of the surrounding nodes.

3.2.4 Comparison of carbon emissions

From the above analysis of CEF index data, it can be seen that by deploying DGs, the carbon emissions cumulated every three hours can be reduced significantly. As can be clearly seen from Figure 8, PV in case 2 does not generate electricity at night, so the cumulated carbon emissions are keep the same as the case 1 with base load only. However, the CHP in case 3 injects the clean power node 10. At 9:00 and 12:00 in the day, the PV output power of case 2 is much larger than the load power of node 10, so the carbon emissions of case 2 at these two time points is the lowest. The results demonstrates that PV plays an important role in reducing carbon emission during the day only,

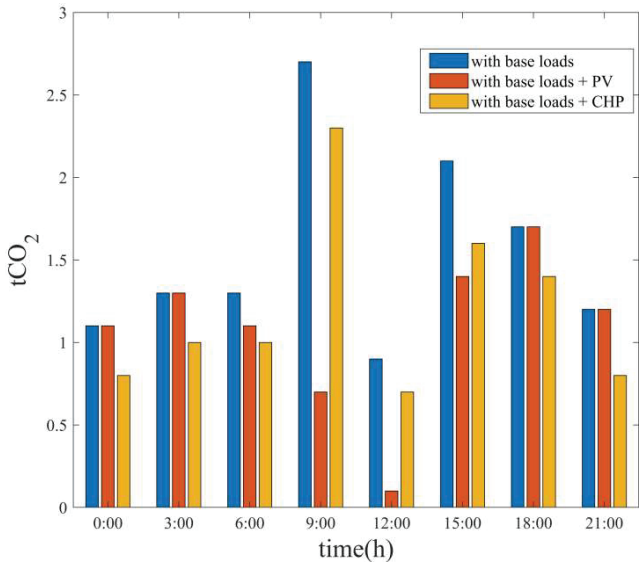

Figure 8 Cumulated carbon emissions of node 10.

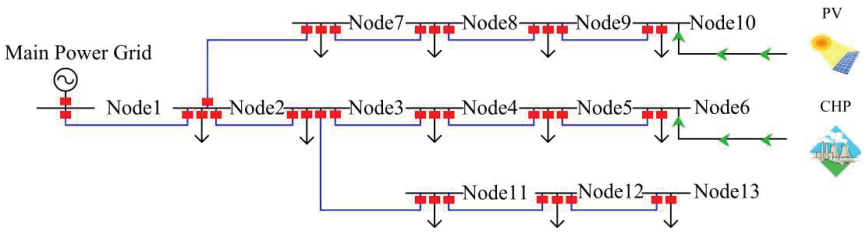

Figure 9 Modified IEEE 13-node system with CHP and PV.

while, CHP as a flexible renewable source, could provide carbon emission through a whole day.

Furthermore, case study 4: Deterministic case with base loads + PV + CHP and the three cases mentioned above are compared to show the number of DGs' impacts on carbon emissions and the more effective in reducing carbon emissions. Since the above three cases consider that a single DG can only reduce the carbon emissions of a particular node or region, ignoring other nodes or regions, there are multiple DGs are deployed in the system.

The carbon emissions of four cases is analyzed based on the same basic data. The carbon emissions in case 2 is set as the benchmark. The comparison results show that coordinated deployment of multiple DGs can reduce carbon emissions more effectively.

Specifically, as shown in Figure 9, adding CHP and PV to node 6 and node 10 respectively, PV affects the region near node 10, and CHP affects the region near node 6. When the power of DGs remains the same, two DGs output power at the same time. The system-wide carbon emissions is shown in Figure 10. In case 4, on one hand, although PV does not generate power at night, but CHP still provides low-carbon power for the system, so the cumulated system-wide carbon emissions are keep the same as the case 3. On the other hand, PV and CHP simultaneously provide low carbon power for the surrounding loads during the day, making the cumulated system-wide carbon emissions reach a minimum during the day, and the cumulated carbon emissions at 9:00, 12:00 and 15:00 are 0.2 t, 0.14 t and 0.6 t lower than those in case 2, respectively.

The cumulated system-wide carbon emissions correspond to the average CI, it can be seen from Figure 11 that with two DGs are deployed, the system-wide average CI in the daytime is cut down considerably. At time of 9:00, the lowest systematic average CI of case 4 is 174gCO_2/kWh lower than that of case 1, demonstrating a dramatic potential on carbon emission reduction impact brought by DGs.

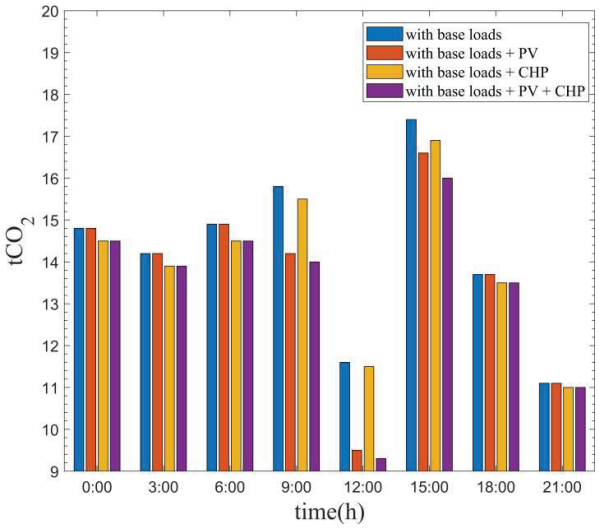

Figure 10 System-wide carbon emissions at different times.

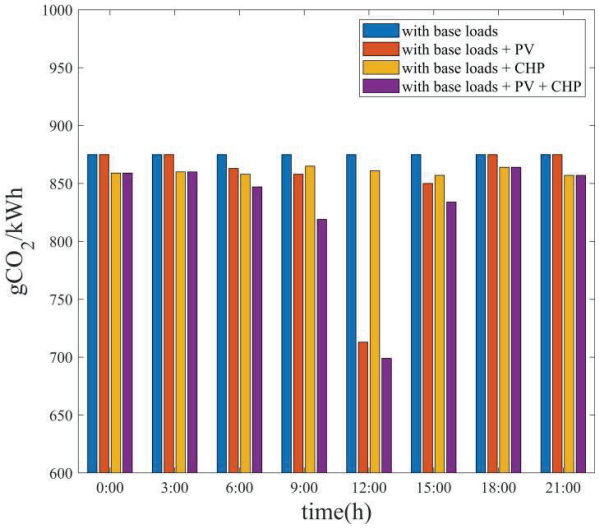

Figure 11 System-wide average CI at different times.

As can be seen from Table 3, total carbon emissions from 12:00 to 13:00 are roughly 9.35t in case 4, which is the lowest among four cases because of the integration of PV and CHP. As per kW power injected by PV, it reduces carbon emissions by 751.2gCO_2. In terms of CHP, it can reduce carbon

Table 3 The systematic average CI by comparing the four cases at 12:00

Case Study	Injected Power at 12:00 (kW)			Average CI (gCO_2/kWh)	Carbon Emission (tCO_2)	Decarbonization (gCO_2/kW)
	Main Power Grid	PV	CHP			
Case 1	13334	0	0	875	11.67	/
Case 2	10434	2900	0	712	9.49	751.2
Case 3	12934	0	400	864	11.53	350
Case 4	10034	2900	400	701	9.35	702.6

emissions by 702.6gCO_2/ kW of power generated. It can be seen that the carbon reduction effect per kW of pure PV is superior to the integration of PV and CHP, with difference of 48.6gCO_2/kW. However, the power production of CHP is more than that of single PV, which leads to the best carbon reduction effect in case 4, with lowest 9.35 t carbon emission only. Thus, it can be seen from the results that deployment of multiple DGs with low CI (such as PV, wind power generation and hydropower) can more effectively reduce carbon emissions, and CHP with relatively high CI can be seen as an reliable energy supplement just in case of power uncertainties brought by renewable power sources.

4 Conclusions

A comprehensive methodology of CEF calculation and analysis in power consuming side is proposed and described in this paper. This method takes into account the CI of DGs and adds the CI of DGs into the calculation of CEF, which can more accurately reflect the carbon emission of the power consuming side, and further highlights the significance of DGs in achieving low-carbon operation. The calculation result show that: (1) The carbon emission trajectory on the power side varies with the power of the DGs. When the electricity provided by the DGs to the neighboring load is far greater than the demand of the load, the excess clean electricity will be transmitted to the nearby area along the distribution network, forming a low-carbon area around the DGs. It provides a factual basis for load environment and technical index in the process of distribution system decarbonization. (2) In the integration of DGs, the carbon emission of the system has been significantly reduced. The simulation also shows that the carbon reduction effect of PV is slightly better than that of CHP. However, due to the characteristics of PV, the

gap between PV and CHP is very small. When PV and CHP are deployed simultaneously in the distribution network, the carbon reduction effect is better than that of single DG. (3) CI and capacity of DG are directly related to carbon emissions. In this paper, the carbon reduction per kW PV is better than the integration of DGs per kW, but limited by the capacity of PV, the final carbon reduction effect of is obvious with the integration of DGs. Deploying multiple high-capacity and low-CI DGs is an option to decarbonize the power sector. This research can further clarify the carbon emission flow in the distribution network in terms of operational level, providing theoretical support for making appropriate renewable energy generation planning and guiding the power system to achieve carbon neutrality.

Acknowledgments

This research is funded by Xiamen University of Technology scientific research project, Research on key technology of "source-network-load" electric-carbon coupling optimized operation in active distribution networks, grant number YKJ22020R and Xiamen Overseas Students Scientific Research Project, Research on low-carbon optimization operation of active distribution networks based on Wind-PV distributed generation, grant number Xia Ren She [2021] No. 207-4).

References

[1] L. Tang et al., "Air pollution emissions from Chinese power plants based on the continuous emission monitoring systems network," Sci Data, vol. 7, no. 1, p. 325, Oct 5 2020. https://www.nature.com/articles/s41597-020-00665-1.

[2] A. Bayu, D. Anteneh, and B. Khan, "Grid Integration of Hybrid Energy System for Distribution Network," Distributed Generation & Alternative Energy Journal, vol. 37, no. 3, pp. 667–675, 12/07 2021. https://doi.org/10.13052/dgaej2156-3306.3738.

[3] S. K. Rajput and D. K. Dheer, "Performance Analysis and Energy Conservation of PV Based Hybrid Power System," Distributed Generation & Alternative Energy Journal, vol. 38, no. 01, pp. 67–84, 12/09 2022. https://doi.org/10.13052/dgaei21563306.3814.

[4] T. Ramanath, D. C. Y. Foo, R. R. Tan, and J. Tan, "Integrated Enterprise Input-Output and Carbon Emission Pinch Analysis for Carbon Intensity

Reduction in Edible Oil Refinery," Chemical Engineering Research and Design, 2023/03/24/ 2023. https://www.sciencedirect.com/science/article/abs/pii/S0263876223001922.

[5] Y. Jiao and D. Månsson, "Greenhouse gas emissions from hybrid energy storage systems in future 100% renewable power systems – A Swedish case based on consequential life cycle assessment," Journal of Energy Storage, vol. 57, p. 106167, 2023/01/01/2023. https://www.sciencedirect.com/science/article/abs/pii/S2352152X22021569.

[6] X. Zhang, Z. Cai, W. Song, and D. Yang, "Mapping the spatial-temporal changes in energy consumption-related carbon emissions in the Beijing-Tianjin-Hebei region via nighttime light data," Sustainable Cities and Society, vol. 94, p. 104476, 2023/07/01/2023. https://www.sciencedirect.com/science/article/abs/pii/S2210670723000872.

[7] Z. Luo et al., "Trade-off between vegetation CO_2 sequestration and fossil fuel-related CO_2 emissions: A case study of the Guangdong–Hong Kong–Macao Greater Bay Area of China," Sustainable Cities and Society, vol. 74, p. 103195, 2021/11/01/ 2021. https://www.sciencedirect.com/science/article/abs/pii/S221067072100473X.

[8] Z. Liu et al., "Carbon Monitor, a near-real-time daily dataset of global CO_2 emission from fossil fuel and cement production," Sci Data, vol. 7, no. 1, p. 392, Nov 9 2020. https://www.nature.com/articles/s41597-020-00708-7.

[9] C. Wang, Z. Lu, and Y. Qiao, "A Consideration of the Wind Power Benefits in Day-Ahead Scheduling of Wind-Coal Intensive Power Systems," IEEE Transactions on Power Systems, vol. 28, no. 1, pp. 236–245, 2013. https://ieeexplore.ieee.org/document/6247491.

[10] T. H. Mehedi, E. Gemechu, and A. Kumar, "Life cycle greenhouse gas emissions and energy footprints of utility-scale solar energy systems," Applied Energy, vol. 314, p. 118918, 2022/05/15/ 2022. https://www.sciencedirect.com/science/article/abs/pii/S0306261922003403.

[11] J. Lu, J. Tang, R. Shan, G. Li, P. Rao, and N. Zhang, "Spatiotemporal analysis of the future carbon footprint of solar electricity in the United States by a dynamic life cycle assessment," iScience, vol. 26, no. 3, p. 106188, 2023/03/17/ 2023.

[12] O. Gavrilova, M. Jonas, K. Erb, and H. Haberl, "International trade and Austria's livestock system: Direct and hidden carbon emission flows associated with production and consumption of products," Ecological Economics, vol. 69, no. 4, pp. 920–929, 2010/02/15/ 2010.

[13] C. Kang et al., "Carbon Emission Flow From Generation to Demand: A Network-Based Model," IEEE Transactions on Smart Grid, vol. 6, no. 5, pp. 2386–2394, 2015. https://ieeexplore.ieee.org/document/7021901.
[14] K. Buayai, K. Chinnabutr, P. Intarawong, and K. Kerdchuen, "Applied MATPOWER for Power System Optimization Research," Energy Procedia, vol. 56, pp. 505–509, 2014/01/01/ 2014. https://www.sciencedirect.com/science/article/pii/S1876610214010479.
[15] H. Saadat.2002. Power Systems Analysis. 2nd. Academic Press, McGraw-Hill Primis Custom Publishing. pp. 150–160.
[16] C. Kang, T. Zhou, Q. Chen, Q. Xu, Q. Xia, and Z. Ji, "Carbon emission flow in networks," Sci Rep, vol. 2, p. 479, 2012. https://www.nature.com/articles/srep00479.
[17] X. Guo, K. Lin, H. Huang, and Y. Li, "Carbon footprint of the photovoltaic power supply chain in China," Journal of Cleaner Production, vol. 233, pp. 626–633, 2019/10/01/ 2019. https://linkinghub.elsevier.com/retrieve/pii/S0959652619320608.
[18] D. R. Subbarao and M. K. Saisarath, "Analysis of a Gas Turbine Plant for Distributed Power Cogeneration Along with Heating, Refrigeration and Air Conditioning," Distributed Generation & Alternative Energy Journal, vol. 32, no. 2, pp. 56–72, 03/09 2017. https://doi.org/10.13052/dgaei21563306.3223.

Biographies

Di Wu graduated from Henan University in 2020. He is currently studying for a master's degree at Xiamen University of Technology. The main research directions include smart distribution grids and low-carbon electricity.

Jun Su graduated in Electrical Engineering from Staffordshire University in 2012 and a master's degree in electrical energy systems from Cardiff University in 2014. 2017.10–2020.12 Studied at Auckland University of Technology, New Zealand, and obtained a PhD in Electrical engineering. 2021.7 Teaching at School of Electrical Engineering and Automation, Xiamen University of Technology. The main research directions include electric vehicles and new energy grid optimization, intelligent distribution network, relay protection.

Zhengyu Chen graduated from Nanjing Institute of Technology in 2020. He is currently studying for a master's degree at Xiamen University of Technology. The main research directions include intelligent distribution network and low-carbon electricity.

Hanhan Liu graduated from North China Institute of Science and Technology in 2021. He is currently studying for a master's degree at Xiamen University of Technology. The main research directions include smart new energy grid optimization and low-carbon electricity.